https://doi.org/10.5194/egusphere-2025-995
Preprint. Discussion started: 29 April 2025
© Author(s) 2025. CC BY 4.0 License.

Modelling the Impacts of Extreme Precipitation Events on Surface Mass Balance in the Eastern Canadian Arctic and Greenland

Nicole A. Loeb[1], Alex Crawford[1], Brice Noël[2], Julienne Stroeve[1,3,4]

[1]Department of Environment & Geography and Centre for Earth Observation Science, University of Manitoba, Winnipeg, MB, Canada
[2] Laboratoire de Climatologie et Topoclimatologie, SPHERES, University of Liège, Liège, Belgium
[3] Department of Earth Sciences, University College London, London, United Kingdom
[4] National Snow and Ice Data Center, Cooperative Institute for Research in Environmental Sciences, University of Colorado Boulder, Boulder, CO, United States

Correspondence to: Nicole A. Loeb (loebn@myumanitoba.ca)

Abstract. Land ice in the Arctic is losing mass as temperatures increase, contributing to global sea level rise. While this loss is largely driven by melt induced by atmospheric warming, precipitation can alter the rate at which loss occurs depending on its intensity and phase. Case studies have illustrated varied potential impacts of extreme precipitation events on the surface mass balance (SMB) of land ice, but the importance of extreme precipitation to seasonal SMB has not been investigated. In this study, simulations from the Regional Atmospheric Climate Model (RACMO) and Variable-Resolution Community Earth System Model (VR-CESM) are explored over historical (1980-1998) and future (2080-2098, SSP5-8.5) periods to reconstruct and further project seasonal SMB for the Greenland Ice Sheet and ice caps of the Eastern Canadian Arctic. Historically, extreme precipitation days consistently had higher SMB than non-extreme precipitation days throughout the study area in both the cold season (DJFM) and warm season (JJAS). In future simulations, this relationship persists for the cold season. However, for the warm season, projections indicate a shift towards less positive and more variable SMB responses to extreme precipitation in the future and extreme precipitation events account for a larger portion of cumulative seasonal positive and negative SMB. Mass loss during extreme precipitation days becomes more common, particularly in SW Greenland and Baffin Island. This likely occurs in part because of a shift toward more rainfall during extreme precipitation events. In other words, in a strong warming scenario, extreme warm season precipitation will no longer reliably yield mass gain for the Greenland Ice Sheet and surrounding ice caps.

1 Introduction

Arctic land ice has been losing mass at an accelerated rate as the climate has warmed (e.g., Hugonnet et al. 2021; Constable et al. 2022). This mass loss is contributing to global sea level rise (e.g., Bamber et al., 2018; Hofer et al., 2020; Jacob et al., 2012) and triggers further warming via the ice-albedo feedback (e.g., Ryan et al., 2023). This ice-albedo feedback is one of the main drivers of "Arctic amplification", which refers to the Arctic region warming approximately four times faster than the global average (Rantanen et al., 2022), in turn enhancing the rate of ice loss. The Greenland Ice Sheet (GrIS) has been one of the largest contributors to global sea level rise since 1900 (van den Broeke et al., 2016; Fettweis et al., 2013; Frederikse et al., 2020; Hofer et al., 2020). A key driver of Greenland's contribution to global sea level rise is increased surface ice melt and

https://doi.org/10.5194/egusphere-2025-995
Preprint. Discussion started: 29 April 2025
© Author(s) 2025. CC BY 4.0 License.

runoff (e.g., Box, 2013; Fettweis et al., 2017). Annual and seasonal surface mass balance (SMB) of the GrIS has been extensively studied through observations (e.g., Bolch et al., 2013; Box, 2013; Cogley, 2004) and modelling (e.g., van Kampenhout et al., 2020; Noël et al., 2018a). The smaller ice caps and glaciers in the eastern Canadian Arctic Archipelago (CAA) have experienced accelerated mass loss in recent decades (Noël et al., 2018b). Lenaerts et al. (2013) showed that 18% of the land ice in the eastern CAA may be lost by 2100, even under a moderate warming scenario.

In models, the SMB is often quantified as

$$SMB = PR - RU - SU - ER \quad (1)$$

where PR refers to precipitation, RU is runoff, SU is loss due to sublimation/phase change, and ER represents wind-driven erosion (Noël et al., 2017, 2018b). The SMB neglects dynamic processes leading to ice loss, such as calving. In general, precipitation is expected to increase in most glaciated regions due to increased water vapour holding capacity (e.g., Bengtsson et al., 2011; Norris et al., 2019; Skific et al., 2009). Surface melt has historically been the dominant factor driving land ice mass loss across much of the Arctic, largely due to rapid temperature increases and relatively low interannual variability in precipitation (Koerner, 2005; Van As et al., 2014). However, as the climate continues to warm, precipitation variability is expected to increase (Pendergrass et al., 2017), suggesting that precipitation may have a more critical impact on the variability of SMB in the future.

The SMB response to precipitation may change as the structure of the firn layer evolves with atmospheric warming. Firn is made up of snow that has lasted at least one melt season but has not yet compacted into glacial ice (Cogley et al., 2011). It is important when considering melt water and liquid precipitation, as it contains interconnected pore spaces that allow for liquid infiltration and freezing/refreezing, resulting in internal accumulation and reducing the amount of mass lost during melt (Forster et al., 2014; van Pelt and Kohler, 2015). However, the firn pore space is limited, and less may be available for retention as more melt and liquid precipitation occur (Machguth et al., 2016; Noël et al., 2022; van Pelt and Kohler, 2015). Noël et al. (2018b) noted how glaciers in the southern CAA are already experiencing decreased refreezing due to the filling of pore spaces, which has also been observed on the GrIS (MacFerrin et al., 2019). In addition to filling firn pore space, intense rainfall events can cause the densification of existing firn and prevent further firn growth (Machguth et al., 2016; Noël et al., 2017), meaning that more surface mass loss may occur due to rainfall in the future.

Another important factor when considering how precipitation may affect SMB is the rate of precipitation. Historical case studies have illustrated how extreme precipitation events can have different impacts depending on the timing and phase of precipitation. During the warm season, intense rainfall events have been shown to dramatically increase runoff and ice discharge (e.g., Doyle et al., 2015), cause the development of ice lenses that prevent infiltration and (re)freezing of liquid water in firn (e.g., Box et al., 2022). Increased surface melt warms the firn as refreezing releases latent heat at depth during infiltration

https://doi.org/10.5194/egusphere-2025-995
Preprint. Discussion started: 29 April 2025
© Author(s) 2025. CC BY 4.0 License.

(e.g., Harper et al., 2023). Doyle et al. (2015) examined rainfall associated with a late summer extratropical cyclone over Western Greenland. The Kangerlussuaq region received approximately 20% of its annual precipitation in a period of seven days, which is very uncommon for the area. This caused a dramatic increase in melt water runoff and acceleration of ice flow. While the cyclone brought warmer temperatures that promoted surface melt, latent heat was released as the rainfall froze to the ice surface, and surface albedo decreased. This caused melt production well into the accumulation region of impacted glaciers. Conversely, a heavy snowfall event during the warm season can increase the albedo and reduce summer melt (e.g., Noël et al., 2015). Oerlemans & Klok (2004) presented observations of a summer snowfall event in the Swiss Alps. An extratropical cyclone caused temperatures to fall by approximately 15°C and a zone of heavy snowfall impacted parts of the Alps for several days. The fresh snowfall led to increased albedo and reduced melt for several days following the event, even when temperatures increased. While extreme precipitation events can cause dramatic short-term SMB changes, their importance in a seasonal context has not been studied.

Climate model simulations project that extreme precipitation events will shift in the future. While mean precipitation is slowly changing, observations have shown that precipitation extremes have shifted more quickly than mean conditions (Fischer and Knutti, 2016; Myhre et al., 2019; Pendergrass et al., 2017). Loeb et al. (2024) showed how extreme precipitation increases across much of the Baffin Bay and Greenland region in simulations of warming scenarios in the Variable-Resolution Community Earth System Model (VR-CESM). Climate model simulations project that a higher portion of annual precipitation will originate from extreme events. One of the factors driving this increase is atmospheric rivers occurring farther north than historically observed (Li & Ding, 2024; Loeb et al., 2024), which can bring high temperatures and extreme precipitation (e.g., Bao et al., 2006; Browning and Pardoe, 1973; Mattingly et al., 2018). Conversely, southeastern Greenland is projected to experience a decrease in the amount of extreme precipitation, likely related to reduced cyclone frequency and intensity in the region (Crawford et al., 2023; Loeb et al., 2024; Priestley and Catto, 2022).

Changing precipitation extremes will impact the rate at which mass loss occurs from the GrIS and ice caps of the eastern Canadian Arctic and therefore may accelerate or decelerate their contributions to sea level rise. While case studies have illustrated the complex impacts of individual extreme precipitation events on the short-term SMB of land ice, the overall importance of extreme events at seasonal time scales has not been investigated. In this study, two climate models are used to investigate the contributions of extreme precipitation events to seasonal and annual SMB of the GrIS and neighbouring ice caps of the eastern Canadian Arctic, and how those contributions differ between historical simulations and climate projections under a high emissions scenario.

https://doi.org/10.5194/egusphere-2025-995
Preprint. Discussion started: 29 April 2025
© Author(s) 2025. CC BY 4.0 License.

2 Data & Methodology

2.1 Model Simulations

2.1.1 Regional Atmospheric Climate Model (RACMO)

The polar version of the Regional Atmospheric Climate Model (RACMO; van Meijgaard et al., 2008) is widely used to investigate the SMB of polar ice sheets (e.g., Lenaerts et al., 2013; Noël et al., 2017, 2018a). It contains a multi-layer snow module (40 layers) that reproduces processes within the snow column, including melt, percolation, refreezing, and runoff (Ettema et al., 2010). The amount of liquid water retention by capillary forces, or irreducible water saturation threshold, is set to 2% in RACMO2.3p2 (Glaude et al., 2024). Parameterization of snow surface albedo is based on prognostic snow-grain size, solar zenith angle, cloud optical thickness, and snow impurities (Kuipers Munneke et al., 2011).

The simulation used here is that of Noël et al. (2020, 2021); RACMO version 2.3p2 is used to dynamically downscale a Coupled Model Intercomparison Project (CMIP6) historical simulation of the Community Earth System Model (CESM) in 1950-2014, followed by a simulation of the SSP5-8.5 scenario in 2015-2100 with a spatial resolution of 11 km. Forcing of atmospheric temperature, pressure, specific humidity, wind speed and direction, sea ice, and sea surface temperature are prescribed at 6-hourly intervals (Noël et al., 2020, 2021).

2.1.2 Variable-resolution Community Earth System Model (VR-CESM)

The National Center for Atmospheric Research's Community Earth System Model (CESM), version 2.2, is a global earth system model that contains component models for the atmosphere, land, ocean, and cryospheric systems (Danabasoglu et al., 2020). The default spatial resolution of CESM is 1° × 1° latitude-longitude (Danabasoglu et al., 2020), but variable-resolution grids have been developed to downscale CESM simulations over areas of interest (Herrington et al., 2022). The Arctic VR-CESM grid is refined to 0.25° × 0.25° latitude-longitude over the entire Arctic nested within the 1° × 1° global simulation (Herrington et al., 2022).

The land component, the Community Land Model, version 5 (CLM5), simulates hydrological and snow processes, including SMB components for grid cells containing land ice (Danabasoglu et al., 2020; Lawrence et al., 2019). The snow cover is modelled with up to 12 layers and may reach a depth of 10 m water equivalent (w.e.) (Lawrence et al., 2019). To account for the complex topography in glaciated areas, each grid cell is divided into 10 elevation classes to adjust atmospheric surface temperature, potential temperature, specific humidity, density, and pressure over ice surfaces (Lawrence et al., 2019). CLM5 also redistributes precipitation produced by the atmospheric component model, the Community Atmosphere Model, version 6 (CAM6) over glaciers. Precipitation is assumed to be snow below -2°C and rainfall above 0°C, with a mix occurring between the two thresholds (Lawrence et al., 2019).

https://doi.org/10.5194/egusphere-2025-995
Preprint. Discussion started: 29 April 2025
© Author(s) 2025. CC BY 4.0 License.

The SMB in CLM5 is calculated as in Eq. 1, except that ER is not explicitly modelled and is therefore not considered (van Kampenhout et al., 2020). Melt is determined based on the surface energy balance calculated over the top few centimeters of snow or ice (van Kampenhout et al., 2020). The snow model within CLM5 contains up to 12 layers, representing up to 10 m of firn or snow (Lawrence et al., 2019). This allows for representation of processes such as compaction and liquid water percolation and retention within the column, with an irreducible water saturation threshold of 3.3% in CLM5 (van Kampenhout et al., 2020). Further details of the calculation of SMB in CLM5 are provided in van Kampenhout et al. (2020). The downscaling of CLM5 within VR-CESM has been shown to improve precipitation rates in the Arctic (Herrington et al., 2022; Loeb et al., 2024) and SMB of the GrIS (van Kampenhout et al., 2019).

Historical (1980-1998; Herrington et al., 2022) and future (2080-2098; Loeb et al., 2024) simulations were completed following the procedure of the Atmospheric Model Intercomparison Project (Hurrell et al., 2008), where the land (CLM5) and atmosphere (CAM6) components are actively modelled and coupled and sea surface temperatures and sea ice conditions are prescribed monthly. Monthly sea ice and sea surface temperatures are retrieved from existing CESM CMIP6 simulations (Danabasoglu et al., 2020; Meehl et al., 2020). The future simulation follows SSP5-8.5.

2.2 Methods

The study domain is divided into nine subregions (Figure 1. Study domain map showing subregions used for analysis.): Canadian subregions are split by island. Greenland is divided into six regions based on glacier regime and SMB characteristics (Rignot et al., 2011; Rignot & Mouginot, 2012). The historical period (HIST) used is 1980-1998 and the future period (FUT) is 2080-2098, limited by the availability of VR-CESM data. Mean annual temperature in the study region rises in FUT relative to HIST by 6.3°C and 7.3°C in RACMO and VR-CESM, respectively. Two seasons are included for analysis: the warm season (JJAS) and cold season (DJFM). Four-month seasons are used, rather than three, to increase the number of extreme precipitation days that can be included for analysis and increase signal-to-noise ratio.

https://doi.org/10.5194/egusphere-2025-995
Preprint. Discussion started: 29 April 2025
© Author(s) 2025. CC BY 4.0 License.

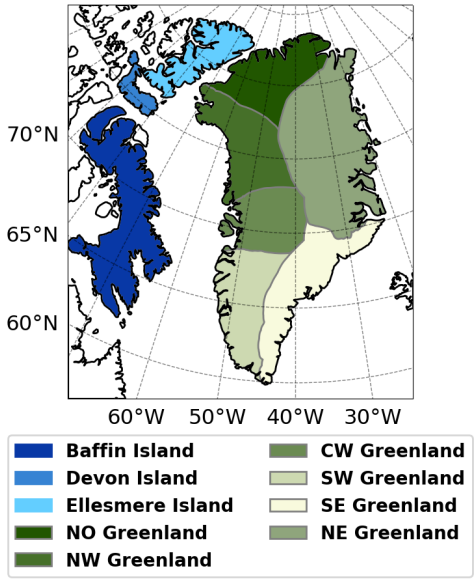

Figure 1. Study domain map showing subregions used for analysis.

Extreme precipitation is defined in two ways for this study: by individual grid cell and by subregion. Extreme precipitation days in each grid cell are those for which total daily precipitation is at or above the 95th percentile of days with at least 1 mm of precipitation, following Loeb et al. (2022, 2024). At the subregion level, extreme precipitation days are defined as the days at or above the 95th percentile of total daily precipitation volume over all grid cells in the subregion. To compare SMB on extreme precipitation days to non-extreme days, non-extreme precipitation days are defined as days where at least half of a region's grid cells receive at least 1 mm of precipitation, but the total amount is less than the extreme threshold for the subregion. In both cases, the historical threshold is used for both periods to assess changes in impacts resulting from precipitation at or above the same threshold. Historical extreme precipitation accumulations are compared to the 5th generation reanalysis product from the European Centre for Medium-Range Weather Forecasts (ERA5; Hersbach et al., 2020) to contextualize historical performance of RACMO and VR-CESM, following Loeb et al. (2024).

SMB anomalies for each extreme precipitation day were calculated relative to a window of ±15 days. We selected this period for anomaly calculation to remove effects of background changes in mean seasonal/annual SMB conditions. Next, the difference between historical and future (FUT minus HIST) interquartile range (IQR_{diff}) of SMB anomalies on extreme precipitation days was calculated. The IQR represents the difference between the first quartile (25th percentile) and third quartile (75th percentile) of the data. To assess statistical significance of this difference, a bootstrapping method was employed in which all years were randomly sorted into two groups and the IQR_{diff} was calculated. Repetitions were performed 1000 times, and if the real IQR_{diff} was greater than (respectively less than) 975 of the tests, this indicated a statistically significant

https://doi.org/10.5194/egusphere-2025-995
Preprint. Discussion started: 29 April 2025
© Author(s) 2025. CC BY 4.0 License.

increase (respectively decrease) in IQR in the future simulation. Note that some of the anomalies from VR-CESM are presented in the supplementary information.

To assess the relative importance of extreme precipitation days to seasonal SMB, we first grouped each day (i) of SMB in each season into positive SMB (SMB_i^+) or negative SMB (SMB_i^-). Second, we calculated the cumulative positive (SMB_{all}^+) and negative SMB (SMB_{all}^-) during a season:

$$SMB_{all}^+ = \sum SMB_i^+ \quad (2)$$

$$SMB_{all}^- = \sum SMB_i^- \quad (3)$$

Third, the same metric was calculated only including extreme precipitation days with positive (negative) SMB for SMB_{ex}^+ (SMB_{ex}^-). Finally, the mean fraction of seasonal positive and negative SMB was calculated as

$$SMB_{ex\ frac}^+ = \frac{SMB_{ex}^+}{SMB_{all}^+} \quad (4)$$

$$SMB_{ex\ frac}^- = \frac{SMB_{ex}^-}{SMB_{all}^-} \quad (5)$$

3 Extreme precipitation

To understand the impacts of extreme precipitation on SMB, we first investigate the occurrence of extreme precipitation and its seasonal and long-term changes. The mean monthly extreme precipitation accumulation in each subregion is shown in Figure 2 to illustrate historical and future conditions across the domain. VR-CESM and RACMO generally agree well with ERA5 in the annual cycle of extreme precipitation over the historical time-period. One exception to this occurs in the winter months in Baffin and Devon Islands, where VR-CESM produces lower extreme precipitation amounts than seen in ERA5 or RACMO.

In all months and regions and for both models, the mean extreme precipitation either remains consistent or increases in the future, with increases to extreme precipitation being most acute in the warm season. Although the two models generally agree about the seasonality of changes, they disagree in SE Greenland, where VR-CESM simulations exhibit little change in any month, but RACMO simulations exhibit a marked increase in warm season extreme precipitation.

https://doi.org/10.5194/egusphere-2025-995
Preprint. Discussion started: 29 April 2025
© Author(s) 2025. CC BY 4.0 License.

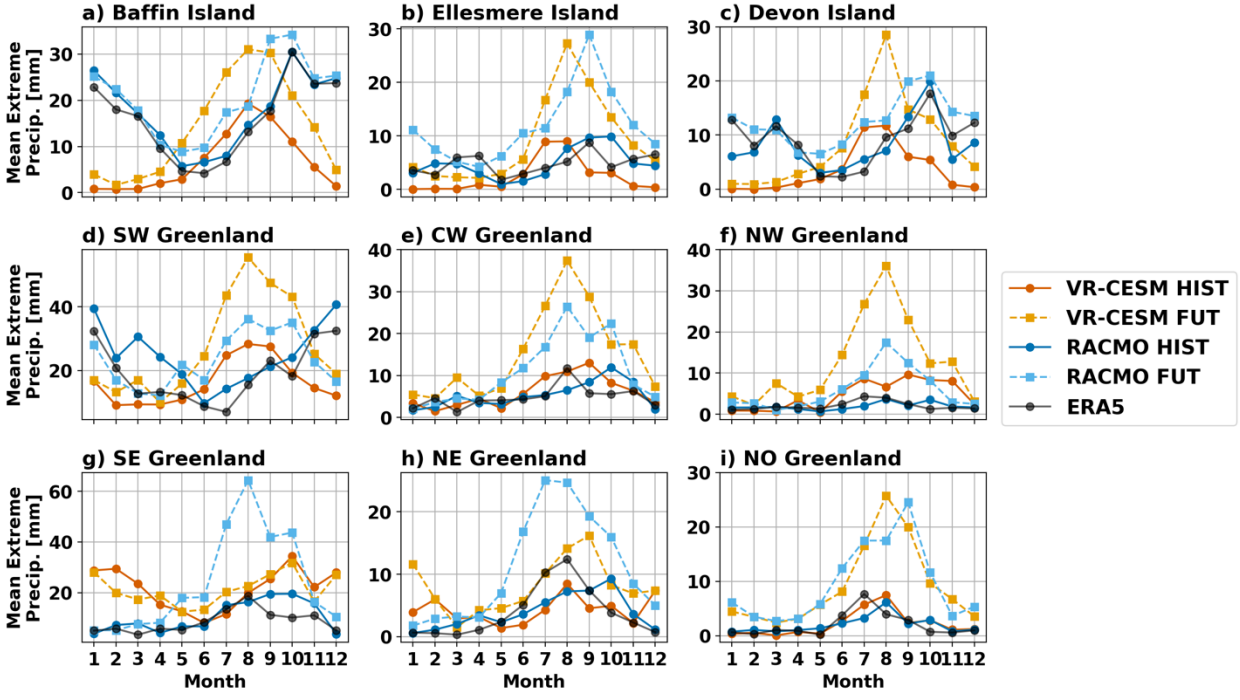

Figure 2. Mean monthly accumulation per grid cell from extreme precipitation in RACMO (blue lines), VR-CESM (orange lines), and ERA5 (black line) for the historical (1980-1998; solid lines) and future (2080-2098; dashed lines) in each subregion.

As outlined in Section 1, whether extreme precipitation falls as rain or snow has major impacts on SMB. Figure 3 shows mean monthly rain fraction of extreme and non-extreme precipitation in each model for the historical and future periods. All subregions show increases in rain fraction in the future, most of which occurs in the warm season. A sharp increase in the rain fraction in June is projected in the Canadian subregions and SW Greenland. Historically, the rain fraction was very similar between extreme and non-extreme precipitation in most subregions. This changes in the future, when several subregions show higher rain fractions on extreme precipitation days than on non-extreme days in the warm season (such as SW, CW, and NW Greenland). Historically, SE Greenland experienced a slightly lower rain fraction for extreme precipitation days than for non-extreme precipitation days in the warm season, but that difference becomes smaller in the future.

https://doi.org/10.5194/egusphere-2025-995
Preprint. Discussion started: 29 April 2025
© Author(s) 2025. CC BY 4.0 License.

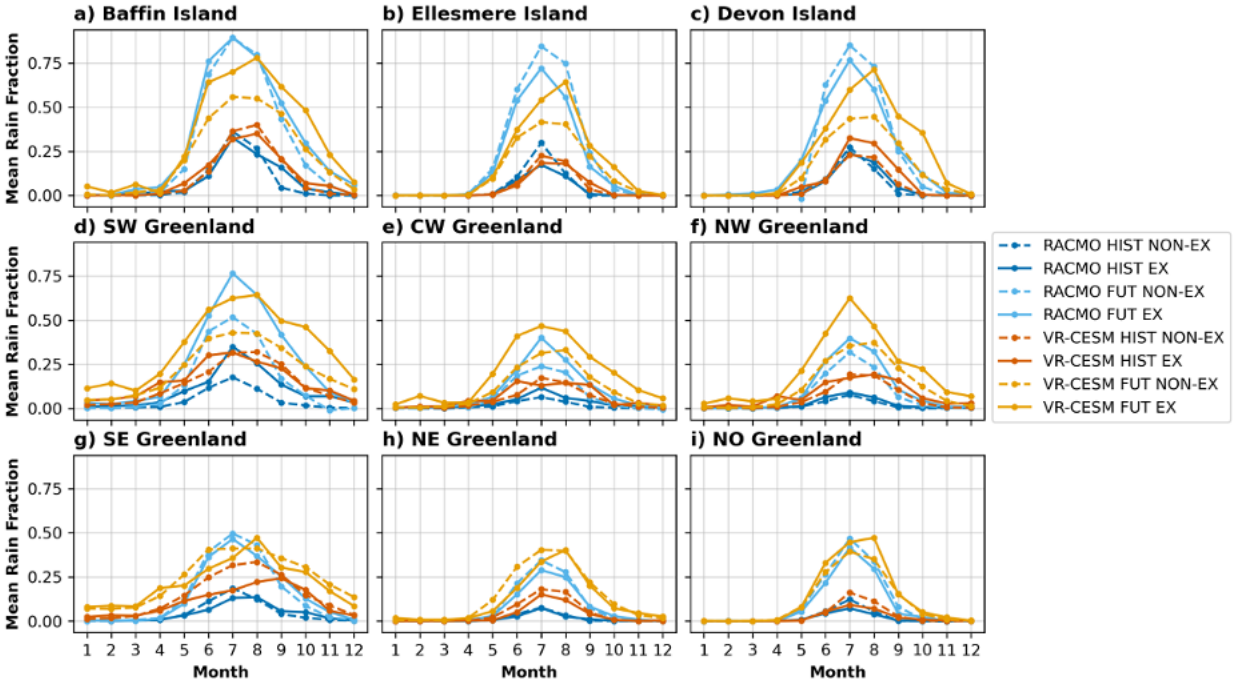

Figure 3. Mean monthly rain fraction for extreme precipitation days (solid lines, "EX") and non-extreme days (dashed lines, "NON-EX") in each subregion (a-i) from RACMO (blue lines) and VR-CESM (orange lines). The darker colours show the historical averages, and the lighter colours show the future projections.

4 SMB Response to Extreme Precipitation

4.1 Mean SMB Responses

Before exploring the impact of extreme precipitation on SMB, we consider mean seasonal SMB in the historical and future RACMO simulations (Figure 4. Mean seasonal SMB in the region for the (a-c) cold season (DJFM) and (d-f) warm season (JJAS) for the historical period (1980-1998; a,d), future period (2080-2098; b,e), and the difference between the two periods (c,f) in RACMO.; VR-CESM shown in Fig. S1). Historically, the cold season (December-March) shows positive SMB across the domain with the highest values in SE Greenland. In the future simulation, we find little change in the mean cold season SMB except for a decrease in SE Greenland. However, SE Greenland still has the highest cold season SMB in the future projections. In the warm season historically, some low-lying and coastal regions show negative seasonal SMB across the domain, but the negative net SMB is limited to narrow margins along the edge of ice masses. In the future projections, the negative seasonal SMB expands to much wider margins of the GrIS, as well as the entirety of the eastern Canadian Arctic.

https://doi.org/10.5194/egusphere-2025-995
Preprint. Discussion started: 29 April 2025
© Author(s) 2025. CC BY 4.0 License.

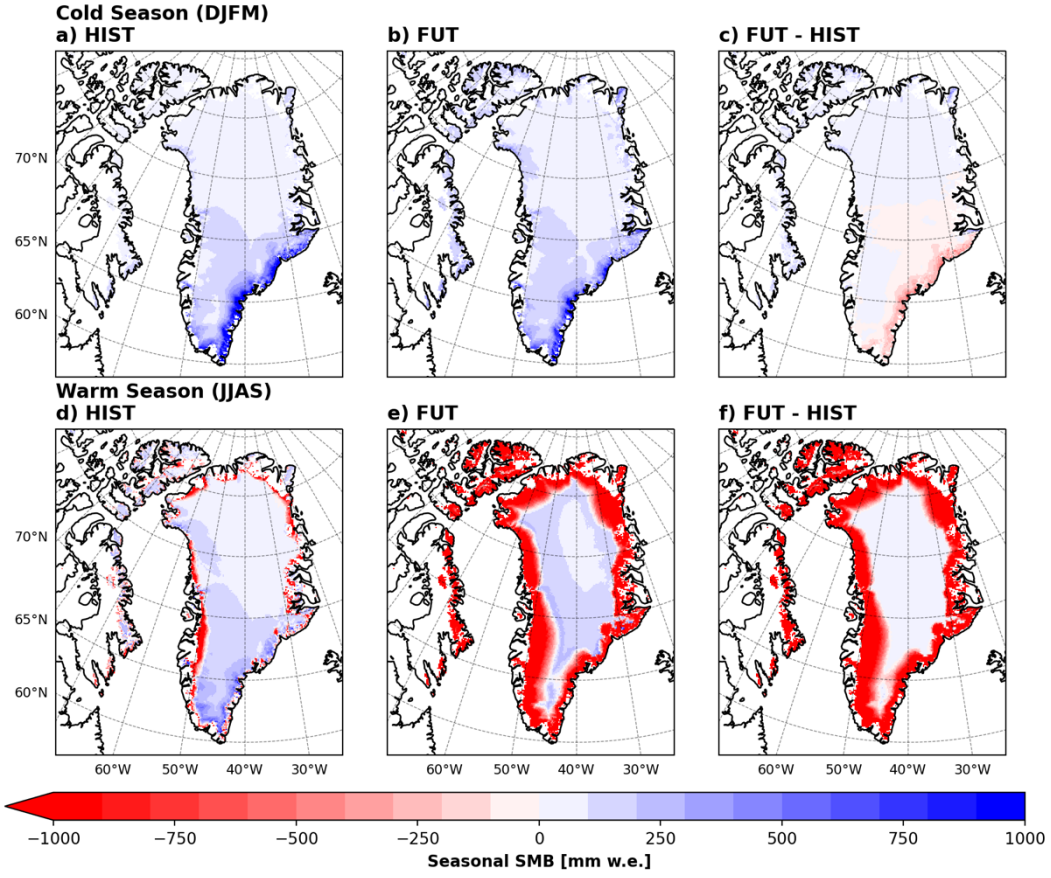

Figure 4. Mean seasonal SMB in the region for the (a-c) cold season (DJFM) and (d-f) warm season (JJAS) for the historical period (1980-1998; a,d), future period (2080-2098; b,e), and the difference between the two periods (c,f) in RACMO.

The average daily SMB on extreme and non-extreme precipitation days in the cold season in each subregion is shown in Figure 5 to understand how extreme precipitation days differ from the average conditions. For all sub-regions, the points for every year lie above the 1:1 line, indicating that SMB is higher on extreme precipitation days than on non-extreme precipitation days. This occurs because the rain fraction is near-zero during the cold season across the domain (Figure 3), so extreme precipitation days represent those when the most mass is added via snowfall. The largest difference between the SMB on extreme and non-extreme precipitation days is found in SW and SE Greenland which have the highest magnitude of extreme precipitation over the cold season (Figure 2).

Most subregions show little consistent change between HIST and FUT in the cold season. VR-CESM shows some general increases in the SMB on extreme precipitation days, particularly in NO Greenland. This is likely due to the increase in the magnitude of extreme precipitation events, as warmer air can hold more moisture (e.g., Bengtsson et al., 2011; Norris et al., 2019; Skific et al., 2009), though only small changes in the magnitude of extreme precipitation are shown in Figure 2. This

https://doi.org/10.5194/egusphere-2025-995
Preprint. Discussion started: 29 April 2025
© Author(s) 2025. CC BY 4.0 License.

difference between HIST and FUT is not as evident in RACMO. There is further disagreement between the models in that VR-CESM produces higher SMB than RACMO in most subregions. Much of this difference may be related to the different spatial resolution of the two models. The slightly coarser resolution of VR-CESM (~ 25 km) compared to RACMO (~ 11 km) allows precipitation to penetrate further inland and affect a larger area. VR-CESM has also been shown to produce higher historical annual SMB for the GrIS compared to RACMO (van Kampenhout et al., 2020), consistent with the differences shown in Figure 5.

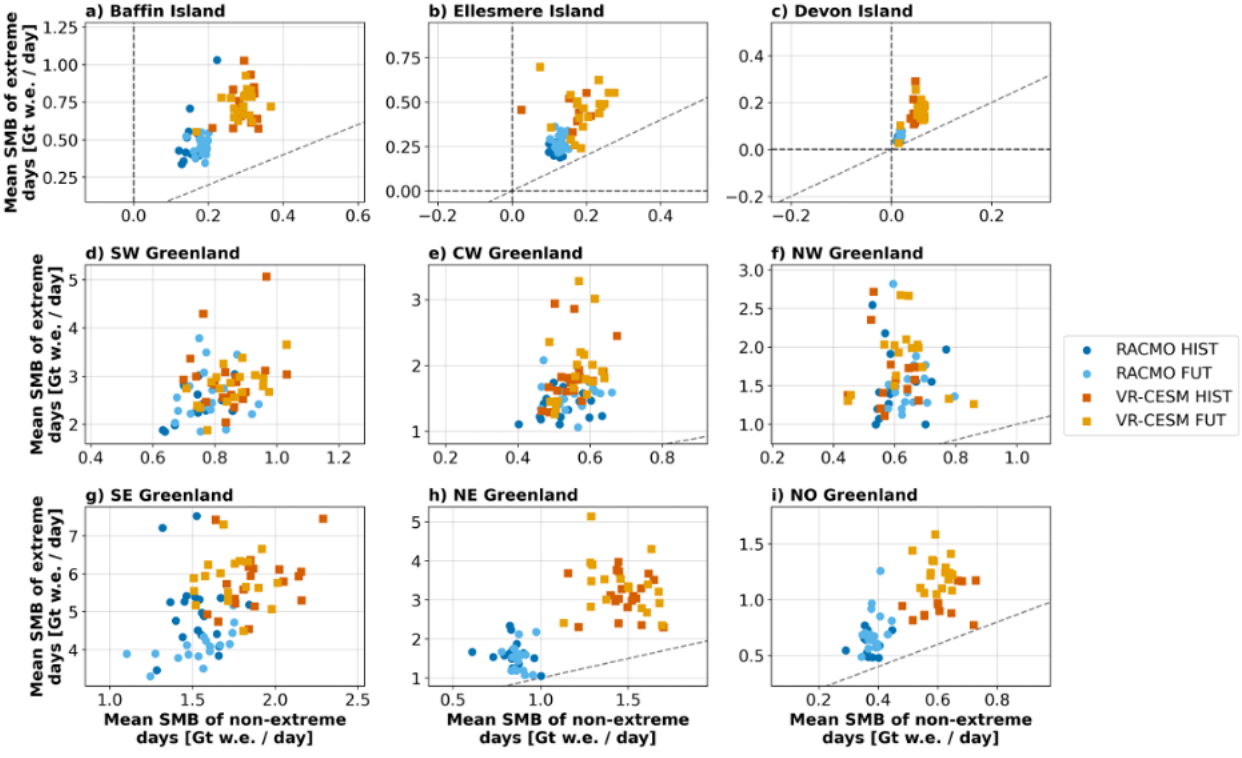

Figure 5. Average DJFM Daily mean SMB on extreme days vs. non-extreme days for all subregions (a-i). Each point represents one year. RACMO is shown in blue circles and VR-CESM is represented by orange/red squares, with the darker (lighter) colour showing historical (future) means. Dashed black lines show x = 0, y = 0, and x = y.

Larger changes in SMB on both extreme and non-extreme precipitation days are projected across the domain during the warm season (Figure 6). Historically, non-extreme precipitation days tended to have SMB near zero or weakly positive, and extreme precipitation days showed positive SMB in all subregions, with strong agreement between the two models. As in the cold season, regional SMB on warm season extreme precipitation days was greater than that of non-extreme days. Historical rain fractions remained near or below 0.25 in the warm season (Fig. 3), meaning that most extreme precipitation events resulted in mass gain via snowfall.

https://doi.org/10.5194/egusphere-2025-995
Preprint. Discussion started: 29 April 2025
© Author(s) 2025. CC BY 4.0 License.

260 However, unlike the cold season, there is a large shift between the historical and future periods in the warm season. In the future projections, the SMB of both extreme and non-extreme days becomes largely negative and more variable as temperatures rise. However, the difference between the SMB on extreme and non-extreme days shifts in many subregions as well. Only SE, CW, NW, and NE Greenland continue to show extreme precipitation days remaining more positive than non-extreme days in the same year. Even in cases where the SMB is more positive on extreme precipitation days than non-extreme days, it is more 265 common in the future for the SMB to be negative, with only NW and SE Greenland usually producing positive SMB on extreme precipitation days. Conversely, SW Greenland and Baffin Island shift more strongly towards extreme precipitation consistently associated with more negative SMB than its non-extreme counterparts, particularly in RACMO.

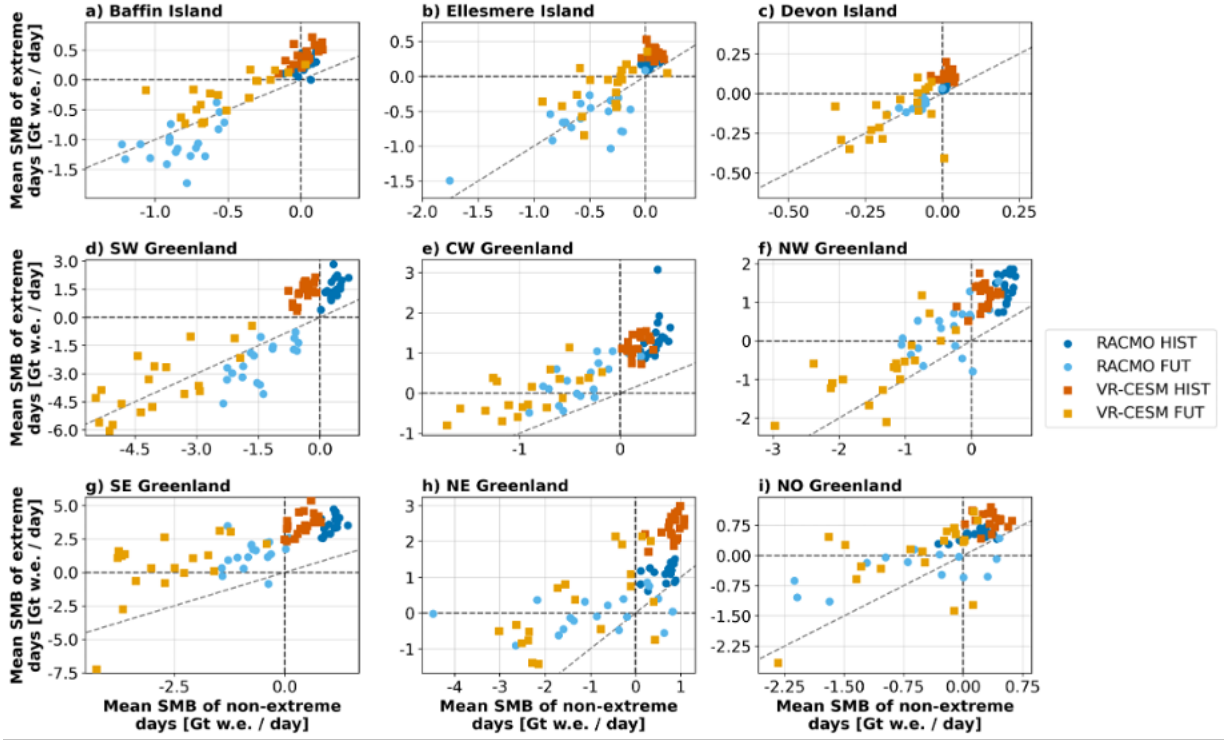

270

Figure 6. As in Fig. 5, but for JJAS.

Historically, the mean SMB of extreme and non-extreme precipitation days were relatively consistent, particularly in the warm season. In the future projections, SMB responses to warm season extreme precipitation days exhibit greater spread and variability (Figure 6). Table 2 and Table 1 show the results of bootstrapping performed on IQR_{diff} in each subregion for the 275 warm and cold seasons, respectively. Both RACMO and VR-CESM show a statistically significant increase in IQR in all subregions except SE Greenland in the warm season. In the cold season, VR-CESM shows an increase in IQR in NW, NE,

https://doi.org/10.5194/egusphere-2025-995
Preprint. Discussion started: 29 April 2025
© Author(s) 2025. CC BY 4.0 License.

and NO Greenland. An increase in NO Greenland is also seen in RACMO, but it shows a decrease in NW and SE Greenland, highlighting the disagreement between the models in the cold season.

Table 1. DJFM IQR bootstrapping results for each subregion. The number of events indicates the total number of extreme precipitation days in DJFM in HIST and FUT. Actual interquartile range (IQR) is the IQR of SMB anomalies on extreme precipitation days in the period and Difference indicates the difference in IQR between the two time periods. Bold indicates a statistically significant change in IQR.

	Subregion	Number of events		Actual IQR *[Gt]*		Difference (FUT-HIST) *[Gt]*
		HIST	FUT	HIST	FUT	
VR-CESM	Baffin Island	29	97	0.208	0.216	0.008
	Ellesmere Island	14	166	0.113	0.229	0.116
	Devon Island	10	108	0.103	0.061	-0.042
	SW Greenland	77	135	1.025	1.065	0.040
	CW Greenland	58	127	0.663	0.780	0.118
	NW Greenland	43	112	0.476	0.837	**0.361**
	SE Greenland	149	139	1.918	2.357	0.438
	NE Greenland	134	172	1.169	1.630	**0.461**
	NO Greenland	30	149	0.199	0.515	**0.316**
RACMO	Baffin Island	31	106	0.166	0.157	-0.009
	Ellesmere Island	16	185	0.061	0.105	0.044
	Devon Island	19	141	0.011	0.027	0.016
	SW Greenland	59	66	0.602	0.976	0.374
	CW Greenland	76	83	0.355	0.584	0.229
	NW Greenland	49	119	0.802	0.366	**-0.436**
	SE Greenland	189	107	2.072	1.121	**-0.951**
	NE Greenland	127	150	0.495	0.607	0.112
	NO Greenland	33	157	0.157	0.308	**0.151**

https://doi.org/10.5194/egusphere-2025-995
Preprint. Discussion started: 29 April 2025
© Author(s) 2025. CC BY 4.0 License.

Table 2. As in Table 1, but for JJAS.

	Subregion	Number of events		Actual IQR *[Gt]*		Difference (FUT-HIST) *[Gt]*
		HIST	FUT	HIST	FUT	
VR-CESM	Baffin Island	184	364	0.389	0.531	**0.142**
	Ellesmere Island	260	465	0.248	0.535	**0.286**
	Devon Island	234	333	0.076	0.198	**0.122**
	SW Greenland	175	309	1.377	3.985	**2.607**
	CW Greenland	164	331	0.678	1.176	**0.498**
	NW Greenland	184	413	0.867	1.368	**0.501**
	SE Greenland	75	85	1.635	2.232	0.597
	NE Greenland	131	255	1.143	1.844	**0.701**
	NO Greenland	236	532	0.442	0.953	**0.511**
RACMO	Baffin Island	194	428	0.236	0.516	**0.280**
	Ellesmere Island	226	531	0.130	0.409	**0.279**
	Devon Island	218	398	0.020	0.084	**0.064**
	SW Greenland	167	358	0.960	2.947	**1.987**
	CW Greenland	129	271	0.547	0.950	**0.403**
	NW Greenland	145	372	0.598	1.280	**0.682**
	SE Greenland	57	88	0.914	1.180	0.266
	NE Greenland	140	407	0.623	1.549	**0.926**
	NO Greenland	203	476	0.395	0.950	**0.555**

Overall, the *IQR* changes shown in Table 2 and Table 1 confirm that the impact of extreme precipitation on SMB changes more in response to warming during the warm season than the cold season. Figure 6In addition to the increased variability, it becomes more common for extreme precipitation to be associated with a negative SMB response in the future (Figure 6). In some subregions, such as NW and CW Greenland, this means that the increased accumulation simply cannot overcome the

https://doi.org/10.5194/egusphere-2025-995
Preprint. Discussion started: 29 April 2025
© Author(s) 2025. CC BY 4.0 License.

strongly negative seasonal SMB. In other regions, such as SW Greenland and Baffin and Ellesmere Islands, this results in extreme precipitation days that are associated with more negative SMB than that of non-extreme days in the future, suggesting that the extreme precipitation days may become particularly detrimental to SMB in the future. These regions also show some of the largest increases in rain fraction (Figure 3). This may help explain the shift towards more negative SMB associated with extreme precipitation, as rainwater directly runs-off on bare ice in ablation zones or progressively saturates firn in accumulation areas. This means that one can no longer assume that extreme precipitation directly leads to mass gain in the future climate.

4.2 Seasonal Context & Change

To contextualize the importance of these events on the seasonal cumulative SMB, seasonal SMB is split into days with positive SMB (SMB^{+}) and negative SMB (SMB^{-}), and the fraction of cumulative positive SMB ($SMB^{+}_{ex\ frac}$) and negative SMB ($SMB^{-}_{ex\ frac}$) that occurs on extreme precipitation days is calculated. The number of extreme precipitation days that occur with positive or negative SMB in each season are shown in Fig. S2. Results from VR-CESM are shown in Figures S3-6, S8-9).

4.2.1 Cold Season

The change in $SMB^{+}_{ex\ frac}$ for DJFM in RACMO is shown in Figure 7 (results from VR-CESM are shown in Fig. S2). Over the historical period, most of the domain received a smaller fraction of positive SMB (<10%) from extreme precipitation days in the cold season, except for SE Greenland (Fig. S2). The $SMB^{+}_{ex\ frac}$ increases slightly in the future across the majority of the domain as extreme precipitation increases (as seen in Figure 2 and Loeb et al., 2024) with the largest $SMB^{+}_{ex\ frac}$ increases occurring at the northernmost areas of Ellesmere Island and NO Greenland. The patterns of changes agree well between RACMO and VR-CESM, although VR-CESM produces higher values of $SMB^{+}_{ex\ frac}$ in NW Greenland. However, SE Greenland shows the opposite: $SMB^{+}_{ex\ frac}$ decreases by approximately 20% in the future projections. This region had the highest historical $SMB^{+}_{ex\ frac}$ due to high extreme precipitation accumulations that peaked in the cold season, but shows decreasing accumulations in the future (Loeb et al., 2024). This is hypothesized to be due to a reduction in extratropical cyclone activity in the region, bringing fewer intense precipitation events to SE Greenland coast (e.g., Crawford et al., 2023; Loeb et al., 2024; Priestley and Catto, 2022). The reduction in $SMB^{+}_{ex\ frac}$ in SE Greenland results in most of the domain showing ~5-10% of seasonal SMB coming from extreme precipitation days in the future.

https://doi.org/10.5194/egusphere-2025-995
Preprint. Discussion started: 29 April 2025
© Author(s) 2025. CC BY 4.0 License.

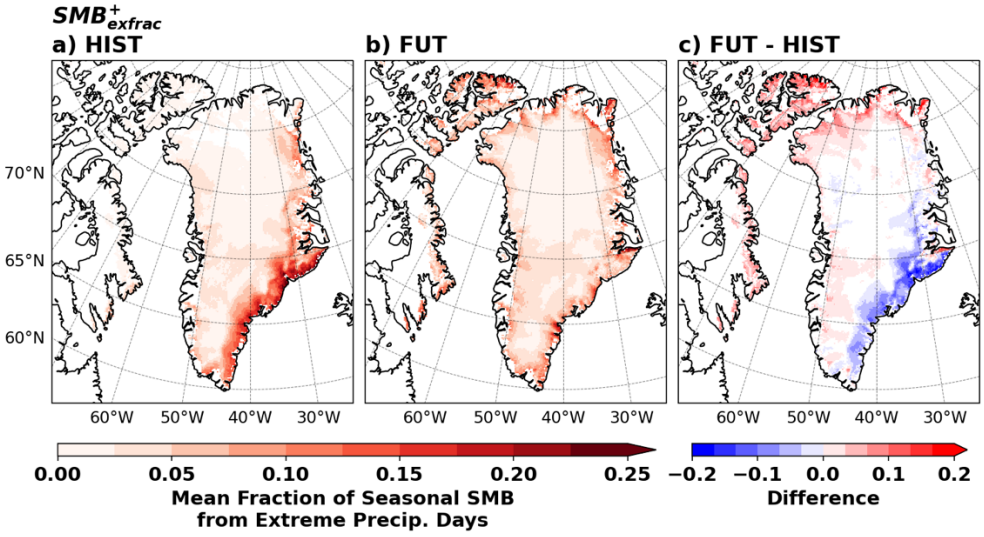

Figure 7. Mean DJFM $SMB^{+}_{ex\,frac}$ from RACMO for HIST (1980-1998; a) and FUT (2080-2098; b). The difference (FUT – HIST) is shown in (c). $SMB^{-}_{ex\,frac}$ is zero across the domain in both periods, and is therefore not shown.

4.2.2 Warm Season

More notable shifts are shown when considering changes in $SMB^{+}_{ex\,frac}$ and $SMB^{-}_{ex\,frac}$ in the warm season (Figure 8, Fig. S4). Historically, $SMB^{-}_{ex\,frac}$ is at or near zero across the domain, with only a small strip of coastal SW Greenland showing ≤ 7% of the negative seasonal SMB coming from extreme precipitation days. Conversely, the entire domain shows 5-20% of positive SMB during the season coming from extreme precipitation days. In the future projections, most of Greenland and northern Ellesmere Island experience an increase in $SMB^{+}_{ex\,frac}$, with extreme precipitation days contributing 10-20% more to the positive SMB in the warm season than in the historical period. The opposite occurs in SW Greenland and Baffin Island, where $SMB^{-}_{ex\,frac}$ increases at the expense of $SMB^{+}_{ex\,frac}$. This suggests a shift in the region, with extreme precipitation days becoming more likely to contribute to seasonal mass loss than mass gain with continued warming. This aligns with the shift towards more negative SMB associated with extreme precipitation shown in Figure 6. In general, RACMO and VR-CESM agree well on the distribution and changes. The increase in $SMB^{-}_{ex\,frac}$ in much of the southern or low altitude regions of the domain Figure 8illustrates how future extreme precipitation days may have more negative contributions to seasonal SMB than shown in the historical period (Figure 8).

https://doi.org/10.5194/egusphere-2025-995
Preprint. Discussion started: 29 April 2025
© Author(s) 2025. CC BY 4.0 License.

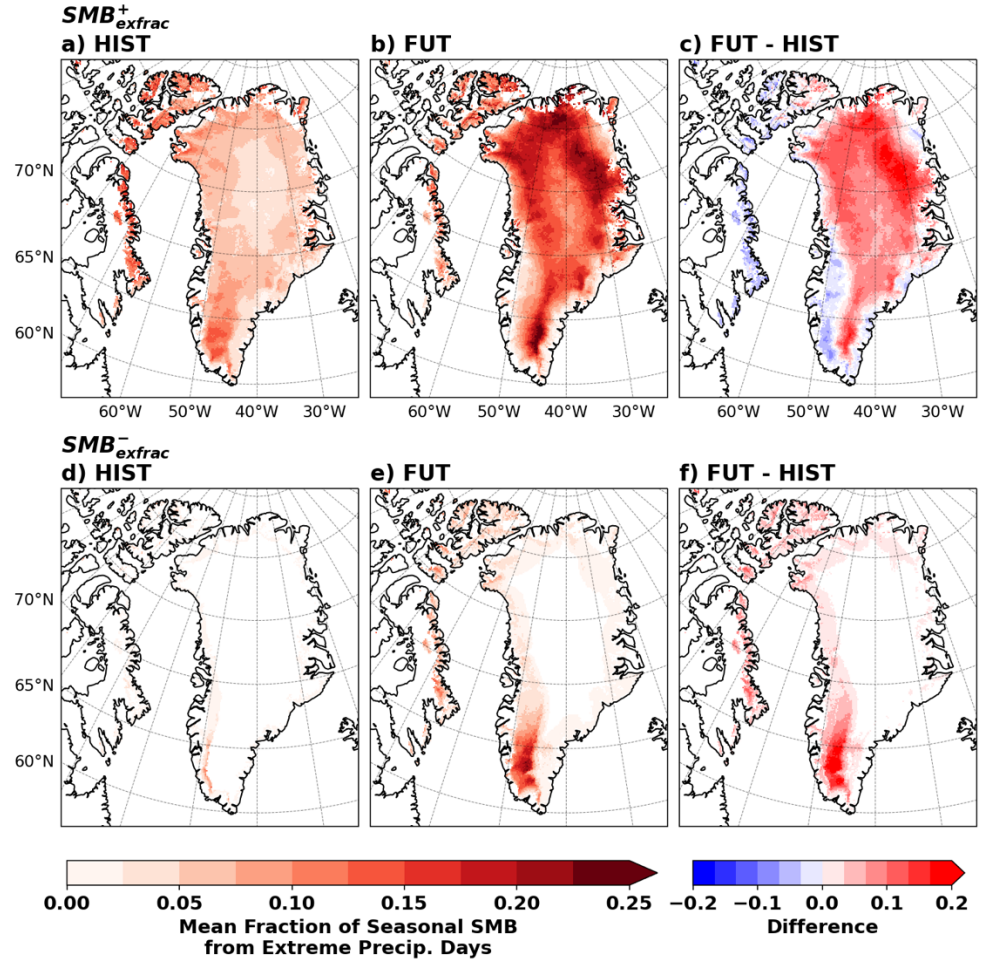

Figure 8. Mean JJAS $SMB^{-}_{ex\,frac}$ (a-c) and $SMB^{+}_{ex\,frac}$ (d-f) from RACMO for HIST (1980-1998; a, d) and FUT (2080-2098; b, e). The difference (FUT – HIST) is shown in (c) and (f) for $SMB^{-}_{ex\,frac}$ and $SMB^{+}_{ex\,frac}$, respectively.

To better understand the impacts of extreme precipitation on SMB components associated with the changes in $SMB^{-}_{ex\,frac}$ and $SMB^{+}_{ex\,frac}$, we explore the mean anomalies associated with warm season extreme precipitation in Figures 9-11. Figure 9Historically, the positive SMB extreme precipitation days generally occur with positive temperature anomalies (~3-4 K) and modest anomalies in melt, runoff, and albedo (Fig. 9). VR-CESM (Fig. S5) shows a slight increase in refreezing occurring on positive SMB extreme precipitation days in SW Greenland. Overall, the models agree on patterns of anomalies, except for albedo, where VR-CESM shows only very small changes.

https://doi.org/10.5194/egusphere-2025-995
Preprint. Discussion started: 29 April 2025
© Author(s) 2025. CC BY 4.0 License.

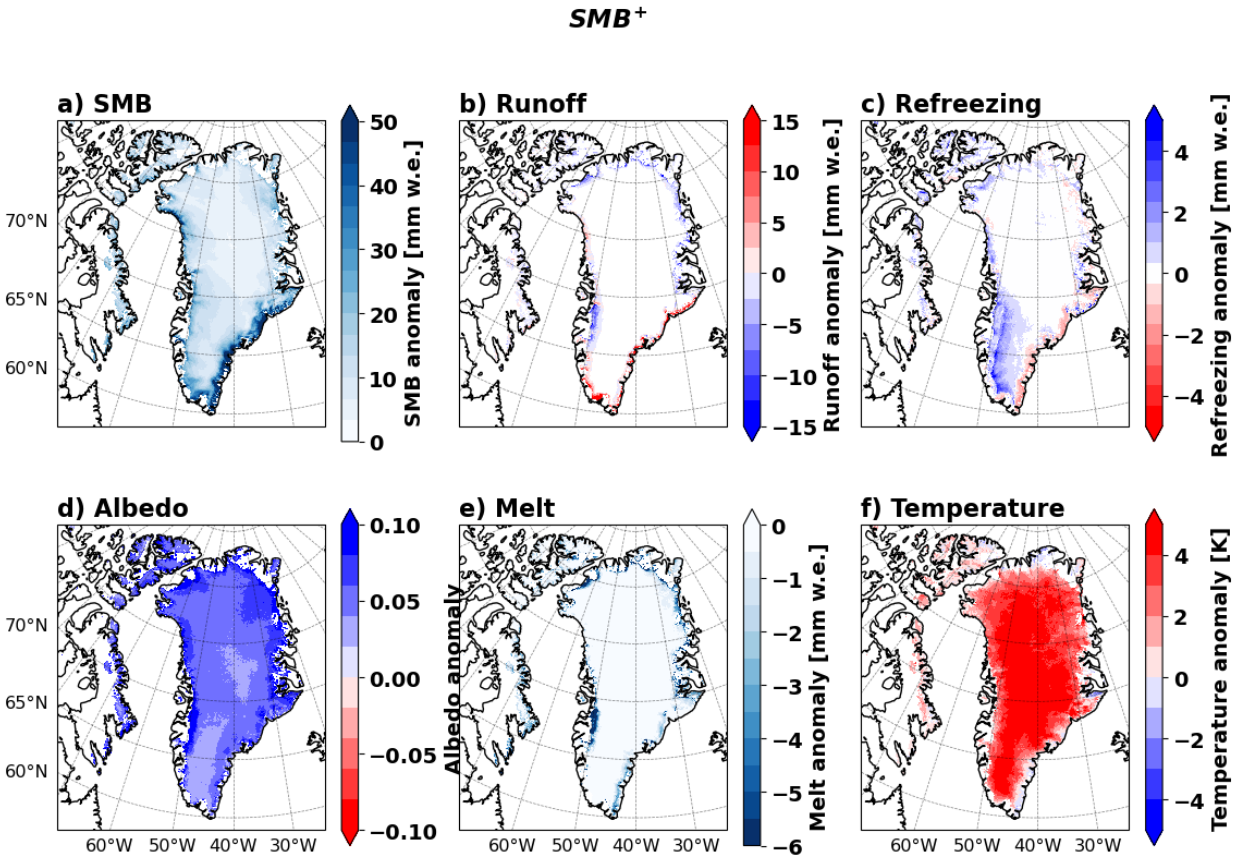

Figure 9. Mean anomalies on positive SMB JJAS extreme precipitation days in the historical period (1980-1998) from RACMO. Anomalies are calculated for the extreme precipitation day relative to ±15 days.

Next, the mean anomalies in future positive SMB extreme precipitation days are illustrated in Figure 10 and S6 from RACMO and VR-CESM, respectively. The models agree well on the patterns of anomalies. One notable change seen in both models is that most inland regions have positive temperature anomalies historically of 2-4 K, but future projections show small negative temperature anomalies (-1 K) in some low-lying and coastal areas. Both models show positive runoff anomalies of approximately 10 mm w.e. on positive SMB extreme precipitation days in SE Greenland. VR-CESM shows modest positive runoff anomalies in Ellesmere and Baffin Islands, disagreeing with the negative anomalies shown in RACMO. However, the largest differences between the models are again seen in the albedo anomalies. RACMO shows relatively large positive albedo anomalies (0.05-0.10) throughout much of the domain with decreased melt whereas VR-CESM shows very low albedo anomalies in general (anomalies below 0.025).

https://doi.org/10.5194/egusphere-2025-995
Preprint. Discussion started: 29 April 2025
© Author(s) 2025. CC BY 4.0 License.

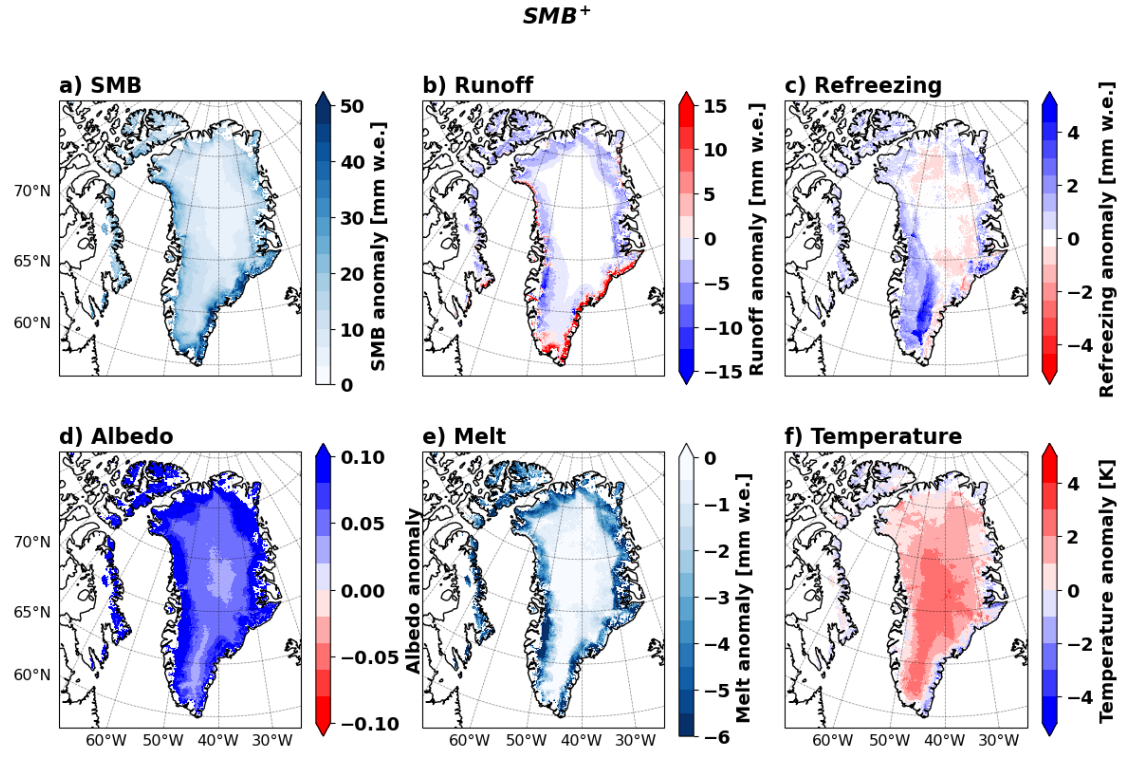

Figure 10. As in Figure 9, but for future (2080-2098) positive SMB JJAS extreme precipitation days from RACMO.

Some of the most notable changes exist in the negative SMB extreme precipitation days, which go from contributing virtually 0% of the SMB^- mass loss historically to approximately 20% in the future period in coastal and southern regions of the domain (Fig. 8). The mean anomalies associated with future events are explored in Figure 11 and S9 from RACMO and VR-CESM, respectively (historical period anomalies are shown in Figures S7-8 as there are few occurrences, as shown in Fig. S2). While the historical simulations had limited events, one notable difference between historical and future simulations is that the temperature anomalies in the historical period (> 4 K; Fig. S7f) tended to be larger than those in the future period (< 2-3 K, and sometimes slightly negative in SE Greenland and Ellesmere Island; Fig. 11f).

Both models show relatively modest SMB anomalies across most of the domain (~-15 mm w.e.), but larger negative anomalies in southern Greenland, occurring with runoff large increases (upwards of 30 mm w.e.). The pattern of refreezing anomalies in each model differs slightly but are relatively small (< 3 mm w.e.). Larger differences exist in albedo anomalies, where VR-CESM is near-zero across the domain and RACMO shows larger negative anomalies in SW Greenland (~-0.10) and positive anomalies along the eastern coast of Greenland (~0.05). RACMO produces much larger positive melt anomalies, which may contribute to the larger decrease in albedo, whereas VR-CESM only shows very localized increases in melt along the coast of SW Greenland. Another notable difference is that the extreme precipitation tends to reach further inland in VR-CESM than

https://doi.org/10.5194/egusphere-2025-995
Preprint. Discussion started: 29 April 2025
© Author(s) 2025. CC BY 4.0 License.

RACMO (e.g., comparing Figures 8d-f to S4d-f), likely owing to the lower resolution producing weaker topography gradients and allowing precipitation to move further inland, as found by van Kampenhout et al. (2020).

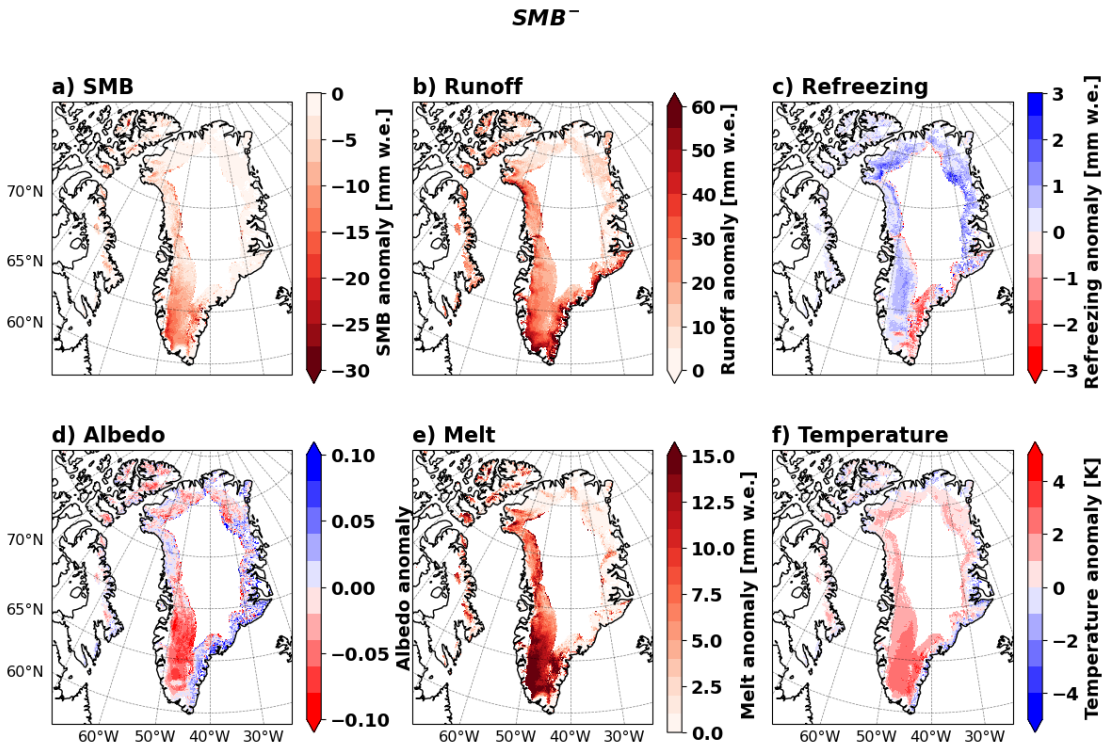

Figure 11. As in Figure 9, but for future negative SMB JJAS extreme precipitation days from RACMO.

In general, the differences in positive SMB extreme precipitation day anomalies between the two time periods are modest. Conversely, the negative SMB extreme precipitation days cause notable anomalies in the future, particularly decreasing the surface albedo in SW Greenland driving prominent increases in melt. In fact, heavy rainfall may alter snow metamorphism to darken the surface, and decreased snowfall increases the period when dark, bare ice is exposed on the surface.

5 Discussion & Limitations

5.1 Connection to previous case studies

As discussed in Section 1, the effects of extreme precipitation on land ice SMB have not been investigated in a climatological context but have been explored in case studies, which can help to contextualize the results found here. Historical positive SMB extreme precipitation days are tied to increases in albedo and refreezing, with less melt occurring, similar to the effect seen by Oerlemans and Klok (2004) in the Swiss Alps. Unlike the case study presented by Oerlemans and Klok (2004), the temperature anomaly associated with warm season positive SMB extreme precipitation days in our study region remains positive during historical positive SMB extreme precipitation days, which is likely due to local climatological factors. The majority of intense

https://doi.org/10.5194/egusphere-2025-995
Preprint. Discussion started: 29 April 2025
© Author(s) 2025. CC BY 4.0 License.

precipitation events in the domain are associated with extratropical cyclones that approach from the south through Baffin Bay or along the North Atlantic Storm Track, bringing warmer air with heavy precipitation (Crawford et al., 2023; Loeb et al., 2024). Because of the high latitude, snowfall can still occur with the warmer air temperatures (Figure 3), leading to overall mass gains. The largest positive temperature anomalies associated with extreme precipitation tend to be at higher altitudes for both positive and negative SMB events.

While historically, there were few negative SMB extreme precipitation days in the warm season, the future impacts align with those seen in recent case studies. Several case studies have noted large runoff anomalies associated with increased melt due to extreme liquid precipitation in the warm season (e.g., Box et al., 2022; Doyle et al., 2015), as seen in Figure 11. Projections suggest that refreezing will begin to decline in the future due to a lack of available firn pore space (Noël et al., 2022), which may contribute to the very modest refreezing anomalies, leading to more liquid water runoff.

5.2 Model albedo differences

Comparing albedo anomalies between RACMO and VR-CESM highlights large differences; RACMO produces anomalies on the order of 0.05-0.1 during extreme precipitation days, whereas those seen in VR-CESM are only ~0.01. These disparities are tied to large differences in the amount of melt that occur, suggesting that the different albedo parameterizations used may be important in understanding the responses. Both models use parts of the Snow, Ice, and Aerosol Radiative (SNICAR) model (Flanner and Zender, 2006) for snow aging metamorphism (van Dalum et al., 2022; Lawrence et al., 2018). However, other aspects of the treatment of albedo differ between the models.

One difference, for example, is the treatment of bare ice. RACMO bases the bare ice albedo on the 500 m MODerate-resolution Imaging Spectroradiometer (MODIS) albedo product, ranging between 0.30 and 0.55 (Noël et al., 2020), whereas VR-CESM assumes bare ice is constant at 0.50 for the visible spectrum (van Kampenhout et al., 2020). Another notable difference is the complexity of the snow module; RACMO can represent a deep snowpack of (up to ~100 m) containing 40 layers (Noël et al., 2020) compared to the maximum depth of ~10 m made up of 12 layers in CLM5 (van Kampenhout et al., 2017, 2020).

Additionally, van Kampenhout et al. (2019) investigated the differences between native resolution CESM and VR-CESM in reproducing historical GrIS SMB and noted several potential biases related to albedo representation. One such issue is that CLM5 repartitions precipitation phase from CAM based on temperature, which does not allow for supercooled rainfall that darkens surface albedo, particularly for the northern GrIS. The downscaling also redistributes clouds within the simulation, which was found to delay summer melt. Additionally, CLM5 does not account for changes in snow properties due to pooling water on the surface, which can lead to darkening being missed by the model. Each of these factors can lead to higher albedos and reduced melt in CLM5, reducing the melt-albedo feedback. This would lead to smaller albedo changes, as seen in Figures S5-6 and S7-8.

https://doi.org/10.5194/egusphere-2025-995
Preprint. Discussion started: 29 April 2025
© Author(s) 2025. CC BY 4.0 License.

Further differences in albedo may arise from the difference in the irreducible water saturation thresholds between the models. While the difference is relatively minor (2% versus 3.3% in RACMO and VR-CESM, respectively), a higher threshold can result in slightly lower runoff occurrence. Even a modest change in simulated runoff can have a variety of impacts, since liquid water at the surface can alter snow metamorphism, albedo, and melt. Glaude et al. (2024) hypothesized this to be a factor in major differences in GrIS SMB projections found from three commonly used regional climate models, including RACMO.

5.3 Limitations

The results presented here help to illustrate the impacts and importance of extreme precipitation events on seasonal SMB, but there are several notable limitations. Firstly, across the domain, it is common for extreme precipitation to occur with warm air advection, driven by features such as atmospheric rivers (e.g., Box et al., 2022; Loeb et al., 2024). Increased air temperature alone can cause increased melt and drive some of the anomalies seen in Section 4. Because of this, it is difficult to disentangle the effects of other climate variables from the effects of extreme precipitation.

Additionally, this analysis only considers impacts on the day of each extreme precipitation event, but the impacts may extend beyond. For example, extreme precipitation events can have direct effects on SMB that last for several days, such as albedo changes (e.g., Oerlemans and Klok, 2004), which may lead to differing seasonal-scale impacts. We also only consider impacts within the area experiencing extreme precipitation, but it is also possible for the precipitation to affect SMB beyond the precipitation area. For example, increased runoff from rainfall and melt can lead to increased melt or refreezing downslope, which would not be accounted for in the current analysis. Future work investigating these extended impacts is necessary to better quantify the true importance of extreme precipitation events.

Finally, only two simulations with relatively short time periods are analyzed in this study, although agreement between the two separate models helps increase confidence in the conclusions. Glaude et al. (2024) illustrated large differences in annual GrIS SMB from three commonly used polar regional climate models using the same forcing data, including the RACMO simulation used in this study. Even though the same CESM2 forcing dataset is used, the three regional models yielded annual SMB that differed by a factor of two, highlighting the importance of looking at a range of projections to understand potential outcomes. RACMO produced the highest future SMB of the three simulations, suggesting that the impacts seen in this study may be more intense in simulations from different polar climate models. Repetition of this assessment with a larger ensemble of high-resolution models with longer simulation periods would be valuable to further substantiate results. It would be particularly insightful to explore models with differing albedo parameterizations to further explore the albedo-related differences seen between RACMO and VR-CESM. Additionally, using higher spatial resolution models may better resolve extreme precipitation events (Ali and Tandon, 2024; Cai et al., 2018) and SMB processes (e.g., Noël et al., 2016).

https://doi.org/10.5194/egusphere-2025-995
Preprint. Discussion started: 29 April 2025
© Author(s) 2025. CC BY 4.0 License.

6 Conclusions

Through the presented analysis of the impacts and importance of extreme precipitation events on the SMB of land ice in Greenland and the Eastern Canadian Arctic, we come to three main conclusions:

Firstly, the changes that occur during the warm season (JJAS) are more prominent than those of the cold season (DJFM), having larger implications for seasonal SMB. Historically, precipitation days in the warm season had positive average SMB in virtually all years and subregions except for SW Greenland and Baffin Island. However, as the climate warms, much of the domain shifts to almost all precipitation days being associated with negative SMB. Even extreme precipitation days are projected to always result in a mean negative seasonal SMB in SW Greenland and the Canadian subregions in the future. There is also a shift in the role that extreme precipitation plays in these subregions in the future. In the historical period, the mean SMB of extreme days was always higher (more positive) than on non-extreme precipitation days. The future projections indicate that this may no longer be the case in SW Greenland and Baffin and Ellesmere Islands, where mean SMB on extreme days becomes even more negative than non-extreme days. This likely results from the shift towards rainfall at the expense of snowfall as temperatures rise. In addition to the potential surface darkening, heavy rainfall can lead to dramatic runoff increases and pooling water that drives further melt. Overall, model projections suggest that extreme precipitation days shift from being contributors of warm season mass gain to a potential driver of sustained mass loss in the future.

Secondly, the relative importance of extreme precipitation days to seasonal SMB is projected to increase in the warm season, with smaller changes occurring during the cold season. The warm season illustrates both positive and negative changes across the domain; extreme precipitation days account for a larger portion of warm season SMB^{+} across inland regions and SMB^{-} in coastal regions, particularly in SW Greenland where the contribution of extreme precipitation days to negative SMB increases from near-zero to approximately 20%. Future changes are generally smaller in the cold season, when the most notable change is a decrease in the contribution of extreme precipitation days to positive SMB in SE Greenland, with small increases across the northernmost regions of the domain where the increased water vapour holding capacity of warmer air allows for more cold season extreme precipitation.

Finally, the SMB responses to warm season extreme precipitation are projected to become more variable in the future. Both models show increases in the IQR of SMB anomalies on extreme precipitation days everywhere except for SE Greenland, where cold season changes are more prominent. The warm season shows the largest projected shift in rainfall fraction. This can drive the more varied SMB impacts in the future since the effects of an extreme event can be dramatically different depending on the precipitation phase. Combined with the shift towards negative SMB, this suggests that one can no longer assume that extreme precipitation simply leads to a mass gain in the region.

https://doi.org/10.5194/egusphere-2025-995
Preprint. Discussion started: 29 April 2025
© Author(s) 2025. CC BY 4.0 License.

This work provides a first estimate of the seasonal-scale impacts of extreme precipitation on the SMB of glaciers and ice caps in the eastern Canadian Arctic and Greenland and how that role may change in the future. While only two models are used in this analysis, it provides a framework for future studies using larger ensembles to further investigate the contribution of extreme precipitation to land ice SMB anomalies under climate warming.

Author contributions

NAL, AC, and JS developed the study and methodology. BN shared RACMO data and guidance on analysis. NAL performed analysis and prepared manuscript. All authors contributed to editing the manuscript.

Acknowledgments

This research was undertaken, in part, thanks to funding from the Canada 150 Research Chairs Program (Grant 50296), the Natural Sciences and Engineering Research Council of Canada (NSERC), and Horizon 2020 CRiceS (Grant 101003826). B. Noël is a Research Associate of the Fonds de la Recherche Scientifique de Belgique – F.R.S.-FNRS. The authors would like to thank Jan Lenaerts and the Land Ice Working Group at the National Center for Atmospheric Research for VR-CESM run support.

References

Ali, S. M. A. and Tandon, N. F.: Influence of Horizontal Model Resolution on the Horizontal Scale of Extreme Precipitation Events, Journal of Geophysical Research: Atmospheres, 129, e2023JD040146, https://doi.org/10.1029/2023JD040146, 2024.

Bamber, J. L., Westaway, R. M., Marzeion, B., and Wouters, B.: The land ice contribution to sea level during the satellite era, Environ. Res. Lett., 13, 063008, https://doi.org/10.1088/1748-9326/aac2f0, 2018.

Bao, J.-W., Michelson, S. A., Neiman, P. J., Ralph, F. M., and Wilczak, J. M.: Interpretation of Enhanced Integrated Water Vapor Bands Associated with Extratropical Cyclones: Their Formation and Connection to Tropical Moisture, Monthly Weather Review, 134, 1063–1080, https://doi.org/10.1175/MWR3123.1, 2006.

Bengtsson, L., Hodges, K. I., Koumoutsaris, S., Zahn, M., and Keenlyside, N.: The changing atmospheric water cycle in Polar Regions in a warmer climate, Tellus A: Dynamic Meteorology and Oceanography, 63, 907–920, https://doi.org/10.1111/j.1600-0870.2011.00534.x, 2011.

https://doi.org/10.5194/egusphere-2025-995
Preprint. Discussion started: 29 April 2025
© Author(s) 2025. CC BY 4.0 License.

Bolch, T., Sandberg Sørensen, L., Simonsen, S. B., Mölg, N., Machguth, H., Rastner, P., and Paul, F.: Mass loss of Greenland's glaciers and ice caps 2003–2008 revealed from ICESat laser altimetry data, Geophysical Research Letters, 40, 875–881, https://doi.org/10.1002/grl.50270, 2013.

Box, J. E.: Greenland Ice Sheet Mass Balance Reconstruction. Part II: Surface Mass Balance (1840–2010), Journal of Climate, 26, 6974–6989, https://doi.org/10.1175/JCLI-D-12-00518.1, 2013.

Box, J. E., Wehrlé, A., van As, D., Fausto, R. S., Kjeldsen, K. K., Dachauer, A., Ahlstrøm, A. P., and Picard, G.: Greenland Ice Sheet Rainfall, Heat and Albedo Feedback Impacts From the Mid-August 2021 Atmospheric River, Geophysical Research Letters, 49, e2021GL097356, https://doi.org/10.1029/2021GL097356, 2022.

van den Broeke, M. R., Enderlin, E. M., Howat, I. M., Kuipers Munneke, P., Noël, B. P. Y., van de Berg, W. J., van Meijgaard, E., and Wouters, B.: On the recent contribution of the Greenland ice sheet to sea level change, The Cryosphere, 10, 1933–1946, https://doi.org/10.5194/tc-10-1933-2016, 2016.

Browning, K. A. and Pardoe, C. W.: Structure of low-level jet streams ahead of mid-latitude cold fronts, Quarterly Journal of the Royal Meteorological Society, 99, 619–638, https://doi.org/10.1002/qj.49709942204, 1973.

Cai, L., Alexeev, V. A., Arp, C. D., Jones, B. M., Liljedahl, A. K., and Gädeke, A.: The Polar WRF Downscaled Historical and Projected Twenty-First Century Climate for the Coast and Foothills of Arctic Alaska, Front. Earth Sci., 5, https://doi.org/10.3389/feart.2017.00111, 2018.

Cogley, J. G.: Greenland accumulation: An error model, Journal of Geophysical Research: Atmospheres, 109, https://doi.org/10.1029/2003JD004449, 2004.

Cogley, J. G., Hock, R., Rasmussen, L. A., Arendt, A. A., Bauder, A., Braithwaite, R. J., Jansson, P., Kaser, G., Möller, M., Nicholson, L., and Zemp, M.: Glossary of Glacier Mass Balance and Related Terms, UNESCO-IHP, Paris, France, 2011.

Constable, A., Harper, S., Dawson, J., Mustonen, T., Piepenburg, D., Rost, B., Bokhorst, S., Boike, J., Cunsolo, A., Derksen, C., Feodoroff, P., Ford, J., Howell, S., Katny, A., MacDonald, J. P., Pedersen, Å. Ø., Robinson, S., Dorough, D. S., Shadrin, V., Skern-Mauritzen, M., Smith, S., Streletskiy, D., Tsujimoto, M., and Dam, B. V.: Cross-Chapter Paper 6: Polar Regions, in: Climate Change 2022: Impacts, Adaptation, and Vulnerability., edited by: Pörtner, H.-O., Roberts, D. C., Tignor, M., Poloczanska, E. S., Mintenbeck, K., Alegría, A., Craig, M., Langsdorf, S., Löschke, S., Möller, V., Okem, A., and Rama, B., Intergovernmental Panel on Climate Change, CCP6-1–66, 2022.

Crawford, A. D., McCrystall, M. R., Lukovich, J. V., and Stroeve, J. C.: The Response of Extratropical Cyclone Propagation in the Northern Hemisphere to Global Warming, Journal of Climate, 36, 7123–7142, https://doi.org/10.1175/JCLI-D-23-0082.1, 2023.

https://doi.org/10.5194/egusphere-2025-995
Preprint. Discussion started: 29 April 2025
© Author(s) 2025. CC BY 4.0 License.

Danabasoglu, G., Lamarque, J.-F., Bacmeister, J., Bailey, D. A., DuVivier, A. K., Edwards, J., Emmons, L. K., Fasullo, J., Garcia, R., Gettelman, A., Hannay, C., Holland, M. M., Large, W. G., Lauritzen, P. H., Lawrence, D. M., Lenaerts, J. T. M., Lindsay, K., Lipscomb, W. H., Mills, M. J., Neale, R., Oleson, K. W., Otto-Bliesner, B., Phillips, A. S., Sacks, W., Tilmes, S., van Kampenhout, L., Vertenstein, M., Bertini, A., Dennis, J., Deser, C., Fischer, C., Fox-Kemper, B., Kay, J. E., Kinnison, D., Kushner, P. J., Larson, V. E., Long, M. C., Mickelson, S., Moore, J. K., Nienhouse, E., Polvani, L., Rasch, P. J., and Strand, W. G.: The Community Earth System Model Version 2 (CESM2), Journal of Advances in Modeling Earth Systems, 12, e2019MS001916, https://doi.org/10.1029/2019MS001916, 2020.

Doyle, S. H., Hubbard, A., van de Wal, R. S. W., Box, J. E., van As, D., Scharrer, K., Meierbachtol, T. W., Smeets, P. C. J. P., Harper, J. T., Johansson, E., Mottram, R. H., Mikkelsen, A. B., Wilhelms, F., Patton, H., Christoffersen, P., and Hubbard, B.: Amplified melt and flow of the Greenland ice sheet driven by late-summer cyclonic rainfall, Nature Geoscience, 8, 647–653, https://doi.org/10.1038/ngeo2482, 2015.

Ettema, J., van den Broeke, M. R., van Meijgaard, E., van de Berg, W. J., Box, J. E., and Steffen, K.: Climate of the Greenland ice sheet using a high-resolution climate model – Part 1: Evaluation, The Cryosphere, 4, 511–527, https://doi.org/10.5194/tc-4-511-2010, 2010.

Fettweis, X., Franco, B., Tedesco, M., van Angelen, J. H., Lenaerts, J. T. M., van den Broeke, M. R., and Gallée, H.: Estimating the Greenland ice sheet surface mass balance contribution to future sea level rise using the regional atmospheric climate model MAR, The Cryosphere, 7, 469–489, https://doi.org/10.5194/tc-7-469-2013, 2013.

Fettweis, X., Box, J. E., Agosta, C., Amory, C., Kittel, C., Lang, C., van As, D., Machguth, H., and Gallée, H.: Reconstructions of the 1900–2015 Greenland ice sheet surface mass balance using the regional climate MAR model, The Cryosphere, 11, 1015–1033, https://doi.org/10.5194/tc-11-1015-2017, 2017.

Fischer, E. M. and Knutti, R.: Observed heavy precipitation increase confirms theory and early models, Nature Clim Change, 6, 986–991, https://doi.org/10.1038/nclimate3110, 2016.

Forster, R. R., Box, J. E., van den Broeke, M. R., Miège, C., Burgess, E. W., van Angelen, J. H., Lenaerts, J. T. M., Koenig, L. S., Paden, J., Lewis, C., Gogineni, S. P., Leuschen, C., and McConnell, J. R.: Extensive liquid meltwater storage in firn within the Greenland ice sheet, Nature Geosci, 7, 95–98, https://doi.org/10.1038/ngeo2043, 2014.

Frederikse, T., Landerer, F., Caron, L., Adhikari, S., Parkes, D., Humphrey, V. W., Dangendorf, S., Hogarth, P., Zanna, L., Cheng, L., and Wu, Y.-H.: The causes of sea-level rise since 1900, Nature, 584, 393–397, https://doi.org/10.1038/s41586-020-2591-3, 2020.

Glaude, Q., Noel, B., Olesen, M., Van den Broeke, M., van de Berg, W. J., Mottram, R., Hansen, N., Delhasse, A., Amory, C., Kittel, C., Goelzer, H., and Fettweis, X.: A Factor Two Difference in 21st-

https://doi.org/10.5194/egusphere-2025-995
Preprint. Discussion started: 29 April 2025
© Author(s) 2025. CC BY 4.0 License.

Century Greenland Ice Sheet Surface Mass Balance Projections From Three Regional Climate Models Under a Strong Warming Scenario (SSP5-8.5), Geophysical Research Letters, 51, e2024GL111902, https://doi.org/10.1029/2024GL111902, 2024.

Herrington, A. R., Lauritzen, P. H., Lofverstrom, M., Lipscomb, W. H., Gettelman, A., and Taylor, M. A.: Impact of grids and dynamical cores in CESM2.2 on the surface mass balance of the Greenland Ice Sheet, Journal of Advances in Modeling Earth Systems, e2022MS003192, https://doi.org/10.1029/2022MS003192, 2022.

Hersbach, H., Bell, B., Berrisford, P., Hirahara, S., Horányi, A., Muñoz-Sabater, J., Nicolas, J., Peubey, C., Radu, R., Schepers, D., Simmons, A., Soci, C., Abdalla, S., Abellan, X., Balsamo, G., Bechtold, P., Biavati, G., Bidlot, J., Bonavita, M., Chiara, G. D., Dahlgren, P., Dee, D., Diamantakis, M., Dragani, R., Flemming, J., Forbes, R., Fuentes, M., Geer, A., Haimberger, L., Healy, S., Hogan, R. J., Hólm, E., Janisková, M., Keeley, S., Laloyaux, P., Lopez, P., Lupu, C., Radnoti, G., Rosnay, P. de, Rozum, I., Vamborg, F., Villaume, S., and Thépaut, J.-N.: The ERA5 global reanalysis, Quarterly Journal of the Royal Meteorological Society, 146, 1999–2049, https://doi.org/10.1002/qj.3803, 2020.

Hofer, S., Lang, C., Amory, C., Kittel, C., Delhasse, A., Tedstone, A., and Fettweis, X.: Greater Greenland Ice Sheet contribution to global sea level rise in CMIP6, Nature Communications, 11, 6289, https://doi.org/10.1038/s41467-020-20011-8, 2020.

Hugonnet, R., McNabb, R., Berthier, E., Menounos, B., Nuth, C., Girod, L., Farinotti, D., Huss, M., Dussaillant, I., Brun, F., and Kääb, A.: Accelerated global glacier mass loss in the early twenty-first century, Nature, 592, 726–731, https://doi.org/10.1038/s41586-021-03436-z, 2021.

Hurrell, J. W., Hack, J. J., Shea, D., Caron, J. M., and Rosinski, J.: A New Sea Surface Temperature and Sea Ice Boundary Dataset for the Community Atmosphere Model, Journal of Climate, 21, 5145–5153, https://doi.org/10.1175/2008JCLI2292.1, 2008.

Jacob, T., Wahr, J., Pfeffer, W. T., and Swenson, S.: Recent contributions of glaciers and ice caps to sea level rise, Nature, 482, 514–518, https://doi.org/10.1038/nature10847, 2012.

van Kampenhout, L., Lenaerts, J. T. M., Lipscomb, W. H., Sacks, W. J., Lawrence, D. M., Slater, A. G., and van den Broeke, M. R.: Improving the Representation of Polar Snow and Firn in the Community Earth System Model, Journal of Advances in Modeling Earth Systems, 9, 2583–2600, https://doi.org/10.1002/2017MS000988, 2017.

van Kampenhout, L., Rhoades, A. M., Herrington, A. R., Zarzycki, C. M., Lenaerts, J. T. M., Sacks, W. J., and van den Broeke, M. R.: Regional grid refinement in an Earth system model: impacts on the simulated Greenland surface mass balance, The Cryosphere, 13, 1547–1564, https://doi.org/10.5194/tc-13-1547-2019, 2019.

https://doi.org/10.5194/egusphere-2025-995
Preprint. Discussion started: 29 April 2025
© Author(s) 2025. CC BY 4.0 License.

van Kampenhout, L., Lenaerts, J. T. M., Lipscomb, W. H., Lhermitte, S., Noël, B., Vizcaíno, M., Sacks, W. J., and van den Broeke, M. R.: Present-Day Greenland Ice Sheet Climate and Surface Mass Balance in CESM2, Journal of Geophysical Research: Earth Surface, 125, e2019JF005318, https://doi.org/10.1029/2019JF005318, 2020.

Kuipers Munneke, P., van den Broeke, M. R., Lenaerts, J. T. M., Flanner, M. G., Gardner, A. S., and van de Berg, W. J.: A new albedo parameterization for use in climate models over the Antarctic ice sheet, J. Geophys. Res., 116, D05114, https://doi.org/10.1029/2010JD015113, 2011.

Lawrence, D. M., Fisher, R. A., Koven, C. D., Oleson, K. W., Swenson, S. C., Bonan, G., Collier, N., Ghimire, B., van Kampenhout, L., Kennedy, D., Kluzek, E., Lawrence, P. J., Li, F., Li, H., Lombardozzi, D., Riley, W. J., Sacks, W. J., Shi, M., Vertenstein, M., Wieder, W. R., Xu, C., Ali, A. A., Badger, A. M., Bisht, G., van den Broeke, M., Brunke, M. A., Burns, S. P., Buzan, J., Clark, M., Craig, A., Dahlin, K., Drewniak, B., Fisher, J. B., Flanner, M., Fox, A. M., Gentine, P., Hoffman, F., Keppel-Aleks, G., Knox, R., Kumar, S., Lenaerts, J., Leung, L. R., Lipscomb, W. H., Lu, Y., Pandey, A., Pelletier, J. D., Perket, J., Randerson, J. T., Ricciuto, D. M., Sanderson, B. M., Slater, A., Subin, Z. M., Tang, J., Thomas, R. Q., Val Martin, M., and Zeng, X.: The Community Land Model Version 5: Description of New Features, Benchmarking, and Impact of Forcing Uncertainty, Journal of Advances in Modeling Earth Systems, 11, 4245–4287, https://doi.org/10.1029/2018MS001583, 2019.

Lenaerts, J. T. M., Angelen, J. H. van, Broeke, M. R. van den, Gardner, A. S., Wouters, B., and Meijgaard, E. van: Irreversible mass loss of Canadian Arctic Archipelago glaciers, Geophysical Research Letters, 40, 870–874, https://doi.org/10.1002/grl.50214, 2013.

Li, Z. and Ding, Q.: A global poleward shift of atmospheric rivers, Science Advances, 10, eadq0604, https://doi.org/10.1126/sciadv.adq0604, 2024.

Loeb, N. A., Crawford, A., Stroeve, J. C., and Hanesiak, J.: Extreme Precipitation in the Eastern Canadian Arctic and Greenland: An Evaluation of Atmospheric Reanalyses, Frontiers in Environmental Science, 10, 2022.

Loeb, N. A., Crawford, A., Herrington, A., McCrystall, M., Stroeve, J., and Hanesiak, J.: Projections and Physical Drivers of Extreme Precipitation in Greenland & Baffin Bay, Journal of Geophysical Research: Atmospheres, 129, e2024JD041375, https://doi.org/10.1029/2024JD041375, 2024.

MacFerrin, M., Machguth, H., As, D. van, Charalampidis, C., Stevens, C. M., Heilig, A., Vandecrux, B., Langen, P. L., Mottram, R., Fettweis, X., Broeke, M. R. van den, Pfeffer, W. T., Moussavi, M. S., and Abdalati, W.: Rapid expansion of Greenland's low-permeability ice slabs, Nature, 573, 403–407, https://doi.org/10.1038/s41586-019-1550-3, 2019.

Machguth, H., MacFerrin, M., van As, D., Box, J. E., Charalampidis, C., Colgan, W., Fausto, R. S., Meijer, H. A. J., Mosley-Thompson, E., and van de Wal, R. S. W.: Greenland meltwater storage in firn

https://doi.org/10.5194/egusphere-2025-995
Preprint. Discussion started: 29 April 2025
© Author(s) 2025. CC BY 4.0 License.

limited by near-surface ice formation, Nature Clim Change, 6, 390–393, https://doi.org/10.1038/nclimate2899, 2016.

Mattingly, K. S., Mote, T. L., and Fettweis, X.: Atmospheric River Impacts on Greenland Ice Sheet Surface Mass Balance, Journal of Geophysical Research: Atmospheres, 123, 8538–8560, https://doi.org/10.1029/2018JD028714, 2018.

Meehl, G. A., Arblaster, J. M., Bates, S., Richter, J. H., Tebaldi, C., Gettelman, A., Medeiros, B., Bacmeister, J., DeRepentigny, P., Rosenbloom, N., Shields, C., Hu, A., Teng, H., Mills, M. J., and Strand, G.: Characteristics of Future Warmer Base States in CESM2, Earth and Space Science, 7, e2020EA001296, https://doi.org/10.1029/2020EA001296, 2020.

van Meijgaard, E., van Ulft, L. H., van den Hurk, B. J. J. M., Lenderink, G., and Siebesma, A. P.: The KNMI regional atmospheric climate model RACMO, version 2., De Bilt, 2008.

Myhre, G., Alterskjær, K., Stjern, C. W., Hodnebrog, Ø., Marelle, L., Samset, B. H., Sillmann, J., Schaller, N., Fischer, E., Schulz, M., and Stohl, A.: Frequency of extreme precipitation increases extensively with event rareness under global warming, Sci Rep, 9, 16063, https://doi.org/10.1038/s41598-019-52277-4, 2019.

Noël, B., van de Berg, W. J., van Meijgaard, E., Kuipers Munneke, P., van de Wal, R. S. W., and van den Broeke, M. R.: Evaluation of the updated regional climate model RACMO2.3: summer snowfall impact on the Greenland Ice Sheet, The Cryosphere, 9, 1831–1844, https://doi.org/10.5194/tc-9-1831-2015, 2015.

Noël, B., van de Berg, W. J., Machguth, H., Lhermitte, S., Howat, I., Fettweis, X., and van den Broeke, M. R.: A daily, 1 km resolution data set of downscaled Greenland ice sheet surface mass balance (1958–2015), The Cryosphere, 10, 2361–2377, https://doi.org/10.5194/tc-10-2361-2016, 2016.

Noël, B., van de Berg, W. J., Lhermitte, S., Wouters, B., Machguth, H., Howat, I., Citterio, M., Moholdt, G., Lenaerts, J. T. M., and van den Broeke, M. R.: A tipping point in refreezing accelerates mass loss of Greenland's glaciers and ice caps, Nat Commun, 8, 14730, https://doi.org/10.1038/ncomms14730, 2017.

Noël, B., van de Berg, W. J., van Wessem, J. M., van Meijgaard, E., van As, D., Lenaerts, J. T. M., Lhermitte, S., Kuipers Munneke, P., Smeets, C. J. P. P., van Ulft, L. H., van de Wal, R. S. W., and van den Broeke, M. R.: Modelling the climate and surface mass balance of polar ice sheets using RACMO2 – Part 1: Greenland (1958–2016), The Cryosphere, 12, 811–831, https://doi.org/10.5194/tc-12-811-2018, 2018a.

Noël, B., van de Berg, W. J., Lhermitte, S., Wouters, B., Schaffer, N., and van den Broeke, M. R.: Six Decades of Glacial Mass Loss in the Canadian Arctic Archipelago, Journal of Geophysical Research: Earth Surface, 123, 1430–1449, https://doi.org/10.1029/2017JF004304, 2018b.

https://doi.org/10.5194/egusphere-2025-995
Preprint. Discussion started: 29 April 2025
© Author(s) 2025. CC BY 4.0 License.

Noël, B., van Kampenhout, L., van de Berg, W. J., Lenaerts, J. T. M., Wouters, B., and van den Broeke, M. R.: Brief communication: CESM2 climate forcing (1950–2014) yields realistic Greenland ice sheet surface mass balance, The Cryosphere, 14, 1425–1435, https://doi.org/10.5194/tc-14-1425-2020, 2020.

Noël, B., Kampenhout, L. van, Lenaerts, J. T. M., van de Berg, W. J., and van den Broeke, M. R.: A 21st Century Warming Threshold for Sustained Greenland Ice Sheet Mass Loss, Geophysical Research Letters, 48, e2020GL090471, https://doi.org/10.1029/2020GL090471, 2021.

Noël, B., Lenaerts, J. T. M., Lipscomb, W. H., Thayer-Calder, K., and van den Broeke, M. R.: Peak refreezing in the Greenland firn layer under future warming scenarios, Nat Commun, 13, 6870, https://doi.org/10.1038/s41467-022-34524-x, 2022.

Norris, J., Chen, G., and Neelin, J. D.: Thermodynamic versus Dynamic Controls on Extreme Precipitation in a Warming Climate from the Community Earth System Model Large Ensemble, Journal of Climate, 32, 1025–1045, https://doi.org/10.1175/JCLI-D-18-0302.1, 2019.

Oerlemans, J. and Klok, E. J. L.: Effect of summer snowfall on glacier mass balance, Annals of Glaciology, 38, 97–100, https://doi.org/10.3189/172756404781815158, 2004.

van Pelt, W. and Kohler, J.: Modelling the long-term mass balance and firn evolution of glaciers around Kongsfjorden, Svalbard, Journal of Glaciology, 61, 731–744, https://doi.org/10.3189/2015JoG14J223, 2015.

Pendergrass, A. G., Knutti, R., Lehner, F., Deser, C., and Sanderson, B. M.: Precipitation variability increases in a warmer climate, Sci Rep, 7, 17966, https://doi.org/10.1038/s41598-017-17966-y, 2017.

Priestley, M. D. K. and Catto, J. L.: Future changes in the extratropical storm tracks and cyclone intensity, wind speed, and structure, Weather and Climate Dynamics, 3, 337–360, https://doi.org/10.5194/wcd-3-337-2022, 2022.

Rantanen, M., Karpechko, A. Y., Lipponen, A., Nordling, K., Hyvärinen, O., Ruosteenoja, K., Vihma, T., and Laaksonen, A.: The Arctic has warmed nearly four times faster than the globe since 1979, Commun Earth Environ, 3, 1–10, https://doi.org/10.1038/s43247-022-00498-3, 2022.

Ryan, J. C., Medley, B., Stevens, C. M., Sutterley, T. C., and Siegfried, M. R.: Role of Snowfall Versus Air Temperatures for Greenland Ice Sheet Melt-Albedo Feedbacks, Earth and Space Science, 10, e2023EA003158, https://doi.org/10.1029/2023EA003158, 2023.

Skific, N., Francis, J. A., and Cassano, J. J.: Attribution of Seasonal and Regional Changes in Arctic Moisture Convergence, Journal of Climate, 22, 5115–5134, https://doi.org/10.1175/2009JCLI2829.1, 2009.